Thermal Degradation of Single-Walled Carbon Nanotubes during Alcohol Catalytic Chemical Vapor Deposition Process

Mohd Asyadi Azam*, Mohd Ambri Mohamed, Eiji Shikoh, and Akihiko Fujiwara
School of Materials Science, Japan Advanced Institute of Science and Technology (JAIST), 1-1 Asahidai, Nomi, Ishikawa 923-1292, Japan

We have grown single-walled carbon nanotubes (SWCNTs) from Co catalyst thin films using the alcohol catalytic chemical vapor deposition (CVD) method for different CVD processing times. The structural properties of the SWCNTs grown have been investigated by Raman spectroscopy with various laser excitations. The growth progressed up to t = 20 min, but the Raman intensity of SWCNTs decreased with increasing CVD processing time. The quality of as-grown SWCNTs also decreased with increasing CVD processing times, similar to the trend for Raman intensity. Raman intensity analysis in the radial breathing mode region shows a relatively wide distribution for SWCNTs grown for all CVD processing times, owing to the variations in growth and burning rates with SWCNT diameter. In this paper, we suggest that Co catalyst poisoning and SWCNT burning occur when the CVD processing time is more than 20 min.

* E-mail address: asyadi@jaist.ac.jp

1. Introduction

Owing to their seamless structure, small diameter, and the resilience of their individual carbon-carbon bonds, carbon nanotubes (CNTs) have extremely high stiffness, strength, and thermal conductivity, [1, 2] which exceed those of all other known natural and synthetic materials. In particular, single-walled carbon nanotubes (SWCNTs) have attracted much attention owing to their novel properties originating from their molecular and electronic structures. Recently, SWCNTs have been more intensively studied than other types of CNT because they exhibit important properties that are not shared by other CNTs.

For the commercialization of CNT products, however, problems or difficulties in the selective growth of SWCNTs abound, such as the extremely high cost of the process and the presence of impurities, usually in the form of catalyst nanoparticles or amorphous carbon, which are formed during the process. Most current growth methods require purification, which results in the degradation of CNTs and again, in a higher cost. However, in 2002, it was reported that high-purity SWCNTs could be grown using ethanol as a low-cost carbon feedstock gas [3], by the so-called alcohol catalytic chemical vapor deposition (ACCVD) method.

With the aim of optimizing high-precision SWCNT growth, or using its directed placement for application in CNT-based field effect transistor (FET) and spin electronic devices, we have performed experimental studies on the growth of SWCNTs from metal catalysts, particularly using low-cost ethanol vapor. [4 - 7] A systematic growth control process was carried out to investigate electronic device characteristics. The optimum growth parameter was selectively determined to be a CVD furnace temperature of 900 ^{o}C, and Co thin films were selected as catalysts with a 1.0 nm nominal thickness, on supporting thin films (100 nm) of Mo. Further intensive experimental studies to achieve more precise growth control remain our main strategy for improving performance.

In this paper, we report one of the controllable factors of SWCNT growth, that is, the CVD processing time, using Co thin films as catalysts. Raman scattering measurements were performed to study the structural changes of SWCNTs grown on the substrates. Although the reaction temperature or gas pressure during growth can change the characteristics or structures of the CNTs grown [8 - 10], CVD processing

time has been considered to mainly affect the amount of CNTs produced. However, in this research, we found that CVD processing time affects not only the amount of SWCNTs grown but also their quality and structure.

2. Experimental Procedure

SWCNTs were grown from a Co catalyst and ethanol vapor via the ACCVD method. [4] A heavily doped n-type silicon wafer ($10 \times 10 \times 0.5$ mm^3) with a 400-nm-thick thermally oxidized SiO_2 layer on its surface was used as the substrate. Co catalyst thin films with a nominal thickness of 1.0 nm were deposited on the substrate by electron-beam deposition. The Co-deposited substrate was subsequently transferred and placed in a CVD reactor. The quartz tube used for the CVD reactor was 1200 mm in length and 26 mm in inner diameter. The reactor was then evacuated using a scroll pump to 0.4 Pa. When the temperature of the movable furnace (heated separately) reached 900 ^{o}C, the furnace was slid to the substrate position. Ar/H_2 (3% H_2) as the pretreatment gas was purged into the reactor at a pressure of 400 Pa concurrently with 7 min rapid heating [11] in order to prevent the oxidation of Co. The Ar/H_2 gas flow was stopped after the furnace temperature returned to 900 ^{o}C, and ethanol vapor was immediately introduced into the reactor at flow rates of 135 – 180 sccm. The initial internal pressure of the CVD reactor during the CVD process was about 2.2 kPa. The CVD processing times (t) for different samples were set to 10, 20, 30, 50, 70, 90, and 115 min. After the CVD process, the furnace was removed from the substrate position, and the ethanol gas flow was stopped. The substrate was left to cool naturally to room temperature.

The SWCNTs grown were characterized using Raman spectroscopy (Tokyo Instruments Nanofinder 30) with three different laser excitations, namely, $\lambda = 441.6$ nm (HeCd), 532.0 nm (Nd:YAG), and 632.8 nm (HeNe), and scanning electron microscopy (SEM; Hitachi S-4100) for morphological study. In the measurements of Raman spectra, the excitation laser spot was focused onto the films formed on the substrate in order to characterize the carbon products. The Raman spectra for the characterization of the products are all measured as for the graphite mode (G-band) intensity being maximum. Recently, it has been found that Raman intensity is very sensitive to the growth direction of CNTs. On the other hand, the absorption of

Raman incident and scattered laser light is almost proportional to the amount of carbon products. Therefore, the excitation laser was focused onto the Si substrate to obtain the maximum Raman intensity of the Si peak, in order to estimate the amount of carbon products from the optical absorption.

3. Results

Figure 1 shows the variation in Raman spectra with CVD processing time (t) measured using all three laser excitations (λ = 441.6, 532.0, and 632.8 nm). The spectra for each CVD processing time are measured at 10 different laser spots taken from the top of the substrate. A blank Si substrate is used as the reference Raman spectrum. All spectra were obtained as for the G-band intensity being maximum, except for that of the blank Si substrate. The Raman spectra and respective baselines are shifted from the bottom (t = 10 min) to the top (t = 115 min) for different CVD processing times. Each sample was continuously measured in sequence from a lower excitation energy to a higher laser excitation energy. The Raman spectra of almost all the samples exhibit peaks of the radial breathing mode (RBM) from 100 to 350 cm^{-1}, which reveal the presence of SWCNTs, a D-band at approximately 1310 cm^{-1}, and a G-band at approximately 1590 cm^{-1}. [12 - 14)]

From Fig. 1, Raman measurement data for t = 20 min shows the highest G-band Raman intensity, among data for all CVD processing times. Most of the SWCNT films grown are still thin (submicron level) compared with vertically aligned SWCNT films. [15 - 18)] From these facts, it is easy to transmit the Raman laser excitation; thus, each spectrum reflects SWCNTs. A clear Si peak for all samples was detected and is shown in Fig. 1. The amount of carbon products will be discussed with the Raman spectra normalized by the maximum Si peak intensity and SEM images.

Figure 2 shows plots of the Raman intensities of the RBM region measured using all laser excitations (extracted from Fig. 1). Analysis in this region shows high absolute Raman intensities for t = 20 and 30 min. RBM Raman signals from 150 to 220 cm^{-1} are observable for almost all measurements. The relationship between the SWCNT diameter and the Raman shift is well described by [19)]

$$\omega_{RBM} = 248/ d_{tube}\,, \qquad (1).$$

where ω_{RBM} is the Raman shift (cm^{-1}) and d_{tube} is the SWCNT diameter. Therefore, we

proposed that the most common diameter of SWCNTs grown in this research is approximately 1.1 – 1.7 nm. The result is consistent with our previous report. [5] In addition, Fig. 3 shows the RBM Raman intensity normalized by the maximum Raman intensity at each measurement. Here, we confirmed a clear variation in the diameter of as-grown SWCNTs, for all CVD processing times in all laser measurements.

Figure 4(a) shows the dependence of the maximum Raman intensity of the G-band for all laser measurements on CVD processing time, extracted from Fig. 1. Excitation lasers were focused onto the products on the substrate during the Raman measurements. The Raman spectra in Fig. 1 clearly indicate very low D-band intensities for all CVD processing times. The G-band to D-band peak intensity ratios, I_G/I_D, for all laser excitations are summarized in Fig. 4(b), and a trend similar to that shown in Fig. 4(a) was confirmed. A high I_G/I_D ratio of up to 21 indicates the relatively good quality [20, 21] of the as-grown SWCNTs. On the other hand, Fig. 4(c) shows the plots of the maximum intensity of the Si peak (same measurement samples) when the lasers were focused onto the substrate during Raman measurements for the estimation of optical absorption by carbon products.

SEM images of the SWCNTs grown for various CVD processing times are shown in Fig. 5. Observations were made from above the substrate and at a tilt angle of 45^o to confirm the formation of a CNT forest on the substrate. When t = 10 to 30 min, SWCNTs tend to form a tangled “spaghetti-like” film on the substrate, indicating the horizontal growth of SWCNTs. Also, in this same time range, most of the areas on the substrates for all CVD processing times show the horizontal growth of SWCNTs. However, it was found that in some areas, a thicker carbon product film (forest) was formed when $t \geq 50$ min. The vertical growth of SWCNTs was observed in some very limited regions, but it was not predominant in contrast to the horizontal growth of SWCNTs. Therefore, a difference in morphology (horizontal or vertical) has only a small effect on the Raman intensity of carbon products measured at all 10 different measurement points. Figure 6 shows a plot of CVD processing time vs the thickness of SWCNT films observed in selected areas on the substrates. The maximum thickness was found to be ~12.6 μm for t = 115 min.

4. Discussion

First, we discuss the quality and approximate quantity of SWCNTs grown during the

CVD process. Although the Raman intensity originating from SWCNTs is not exactly proportional to the actual quantity grown on the substrate, we can roughly estimate the quantity from the intensity of SWCNTs, because most SWCNTs are horizontally aligned for all CVD processing times. In this research work, we obtain relatively high values of I_G/I_D, especially for t = 20 min. This result also corresponds to the strong Raman RBM and G-band peak intensities, and is consistent with the quality of SWCNTs grown. SWCNTs can be effectively grown using this system (technique) with t = 20 min.

With increasing CVD processing time, the Raman intensity of carbon products decreased. The Si peak intensity also decreased with increasing t, which means that the absorption of laser light by carbon products increased. Furthermore, from SEM, we found that the SWCNT bundle size slightly increased at t = 30 min compared with those at t = 10 and 20 min, and became significantly larger for longer CVD processing times. This result can also be attributed to the formation of defective by-products or amorphous carbon [22], which is directly responsible for the decrease in the quality for longer CVD processing times and the increase in optical absorption induced by carbon products. It should be noted again that the vertical growth of SWCNTs is not predominant on the substrate, and therefore does not markedly affect influence the optical absorption by carbon products.

From the above results, we propose that the effective growth of high-quality SWCNTs can be achieved with CVD processing times of up to 30 min. After that, the amount of defects or amorphous carbon increases, as a result of catalyst poisoning and CNT burning for longer CVD processing times. [23] Some form of catalyst poisoning may be due to the formation of a carbonaceous layer around catalyst nanoparticles, and the cause of SWCNT burning can be attributed to oxidation reactions activated by H_2O and/or dissociated from ethanol. [23, 24]

The Raman analysis of the RBM region showed that the relative intensity of the SWCNTs grown remained at the same Raman shift from t = 10 min to t = 115 min. However, the RBM peak intensity trend at all t changes with Raman laser excitation. The strongest peak intensities for 441.6 and 532.0 nm laser excitations are slightly shifted to lower Raman shift; however, the RBM peak intensities for 632.8 nm laser excitation show the reverse result, especially for longer CVD processing times. It is presumed that the Raman intensity in the RBM region shows similar trends for all laser excitations. The changes are possibly due to the interfusion or mixture of

SWCNT growth, burning, and the production of impurities during the CVD process. This fact is also related to the changes (decay) in the quality and purity of as-grown SWCNTs. The variation in the relative diameter distribution may be attributed to the differences in growth and burning rates due to a difference in SWCNT diameter. On the other hand, for the catalytic CVD process of SWCNTs, it is well-known that the SWCNT diameter also correlates strongly with the size of metal catalyst nanoparticles. Thus, by controlling the size of catalyst nanoparticles, one should be able to control the SWCNT diameter. [8] However, under severe conditions for SWCNT growth at relatively high reaction temperatures, it is difficult to maintain fine control over the catalyst particle size, owing to the inevitable thermal sintering. [25] For our CVD system conditions with a relatively high reaction temperature (900 ^{o}C), the diameters of Co nanoparticles were distributed from 1 to 11 nm. [26] This wide range of diameters might also be responsible for the wide range of SWCNT diameter distributions.

5. Conclusions

We have investigated the SWCNT growth from Co catalyst thin films (1.0 nm nominal thickness before growth) at 900 ^{o}C using the alcohol catalytic CVD method. The quality and quantity of as-grown SWCNTs were determined using Raman scattering measurement with different laser excitations. It was confirmed that SWCNTs can be effectively grown using this system (technique) when t = 20 min. The increase in the amount of impurities (defects, and amorphous carbon) and the formation of larger SWCNT bundles for longer CVD processing times are responsible for the decrease in Raman peak intensity. Furthermore, relative RBM intensity analysis shows a wide distribution of the diameters of SWCNTs grown at all CVD processing times due to the variation in growth and burning rates with SWCNT diameter. This result is related to catalyst poisoning, and SWCNT burning, which may have occurred for longer CVD processing times (more than 20 min). In this paper, we suggest that CVD processing time is another key factor affecting the characteristics of SWCNTs grown by the ACCVD method.

Acknowledgements

This work was supported by a Grant-in-Aid (Grant No. 20048001) of “Carbon Nanotube Nano-Electronics” for Scientific Research on the Priority Area from the Ministry of Education, Culture, Sports, Science and Technology, Japan (MEXT). Part of this work was conducted in Kyoto-Advanced Nanotechnology Network, also supported by MEXT.

1. MatWebMaterial Property Data, [http://www.matweb.com].
2. US National Materials Advisory Board: National Academy of Sciences Tech. Rep. (2005).
3. S. Maruyama, R. Kojima, Y. Miyauchi, S. Chiashi, and M. Kohno: Chem. Phys. Lett. **360** (2002) 229.
4. N. Inami, M. A. Mohamed, E. Shikoh, and A. Fujiwara: Sci. Tech. Adv. Mater. **8** (2007) 292.
5. N. Inami, M. A. Mohamed, E. Shikoh, and A. Fujiwara: Appl. Phys. Lett. **92** (2008) 243115.
6. M. A. Mohamed, N. Inami, E. Shikoh, Y. Yamamoto, H. Hori, and A. Fujiwara: Sci. Technol. Adv. Mater. **9** (2008) 025019.
7. M. A. Mohamed, M. A. Azam, E. Shikoh, and A. Fujiwara: to be published in Jpn. J. Appl. Phys.
8. H. Sugime, S. Noda, S. Maruyama, and Y. Yamaguchi: Carbon **47** (2009) 234.
9. W. L. Wang, X. D. Bai, Z. Xu, S. Liu, and E. G. Wang: Chem. Phys. Lett. **419** (2005) 81.
10. W. Z. Li, J. G. Wen, and Z. F. Ren: Appl. Phys. A **74** (2002) 397.
11. S. Huang, M. Woodson, R. Smalley, and J. Liu: Nano Lett. **4** (2004) 1025.
12. R. Saito, G. Dresselhaus, and M. S. Dresselhaus: *Physical Properties of Carbon Nanotubes* (Imperial College Press, London, 1998) Chap. 10, p.183.
13. M. S. Dresselhaus, and P. C. Eklund: Adv. Phys. **49** (2000) 705.
14. M. S. Dresselhaus, G. Dresselhaus, R. Saito, and A. Jorio: Phys. Rep. **409** (2005) 47.
15. S. Maruyama, E. Einarsson, Y. Murakami, and T. Edamura: Chem. Phys. Lett. **403** (2005) 320.
16. K. Hata, D. N. Futaba, K. Mizuno, T. Namai, M. Yumura, and S. Iijima: Science **306** (2004) 1362.
17. S. Noda, K. Hasegawa, H. Sugime, K. Kakehi, Z. Zhang, S. Maruyama, and Y. Yamaguchi: Jpn. J. Appl. Phys. **46** (2007) 399.
18. H. Ohno, D. Takagi, K. Yamada, S. Chiashi, A. Tokura, and Y. Homma: Jpn. J. Appl. Phys. **47** (2008) 1956.
19. A. Jorio, R. Saito, J. H. Hafner, C. M. Lieber, M. Hunter, T. McClure, G. Dresselhaus, and M. S. Dresselhaus: Phys. Rev. Lett. **86** (2001) 1118.

20. C. C. Chiu, C. Y. Chen, N. Y. Tai, and C. H. Tsai: Surf. Coat. Technol. **200** (2006) 3199.
21. S. Arepalli, P. Nikolaev, O. Gorelik, V. G. Hadjiev, W. Holmes, B. Files, and L. Yowell: Carbon **42** (2004) 1783.
22. A. Jorio, M. A. Pimenta, A. G. Souza Filho, R. Saito, G. Dresselhaus, and M. S. Dresselhaus: New J. Phys. **5** (2003) 139.
23. E. Einarsson, Y. Murakami, M. Kadowaki, and S. Maruyama: Carbon **46** (2008) 923.
24. H. Yan, Q. Li, J. Zhang, and Z. Liu: Carbon **40** (2002) 2693.
25. W. L. Wang, X. D. Bai, Z. Xu, S. Liu, and E. G. Wang: Chem. Phys. Lett. **419** (2006) 81.
26. N. Inami: Dr. Thesis, School of Materials Science, Japan Advanced Institute of Science and Technology, Ishikawa (2008).

Figure captions

Fig. 1. (Color online) Raman spectra of the blank substrate, and samples with CVD processing times of 10, 20, 30, 50, 70, 90, and 115 min measured using three laser excitations (λ = 441.6, 532.0, and 632.8 nm). The Raman spectra were measured from 10 different laser spots. Peaks at approximately 303, 520, and 960 cm^{-1} are from the Si/SiO_2 substrate, and can be used for x-axis calibration purposes. The Raman spectra and respective baselines are shifted vertically for all laser excitations for clarity.

Fig. 2. (Color online) Absolute Raman intensities of RBM region measured for all laser excitations extracted from Fig. 1. All measurements were performed using the same parameters, at room temperature. Note that the CVD processing time, *t* ranges from 10 to 115 min. The Raman spectra and respective baselines are shifted vertically for all laser excitations for clarity.

Fig. 3. (Color online) Raman intensities of RBM region normalized by maximum intensity measured for all laser excitations. Note that the CVD processing time *t* ranges from 10 to 115 min. The Raman spectra and respective baselines are shifted vertically by one intensity value in all laser measurements.

Fig. 4. (Color online) (a) Peak intensity of G-band with the laser focused onto the products on the substrate for all measurements. (b) Comparison of I_G/I_D ratios for SWCNTs grown at different *t*, measured using all laser excitations. I_G and I_D correspond respectively to the Raman intensities of the D-band and G-band regions in Raman spectra. (c) Si peak intensity when the laser was focused onto the substrate.

Fig. 5. SEM images of SWCNTs grown on the substrate for CVD processing times, *t* = 10 min – 115 min. Left images were taken from above the substrate, and the right images were taken at a tilt angle of 45^o.

Fig. 6. (Color online) Thicknesses of vertical growth areas on the substrate for all CVD processing times, confirmed by SEM observation at tilt angle of 45^o.

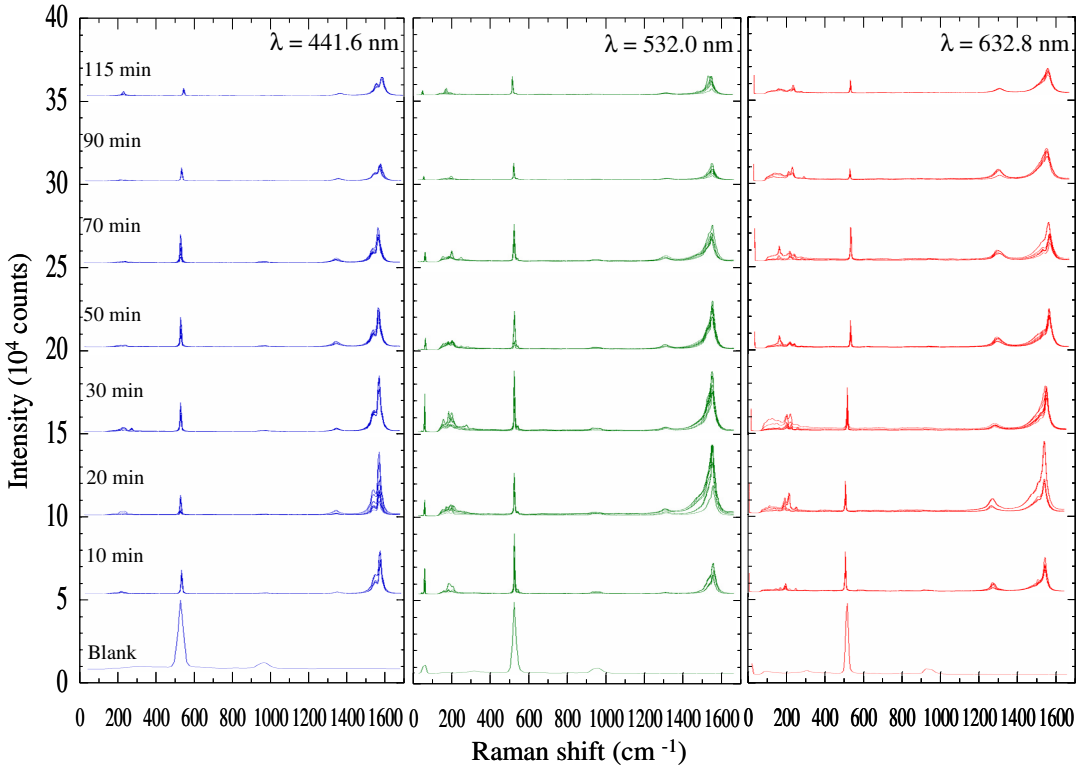
λ = 441.6 nm
λ = 532.0 nm
λ = 632.8 nm
115 min
90 min
70 min
50 min
30 min
20 min
10 min
Blank
Intensity (10⁴ counts)
Raman shift (cm -1)
0
5
10
15
20
25
30
35
40
0 200 400 600 800 1000 1200 1400 1600

Fig. 1

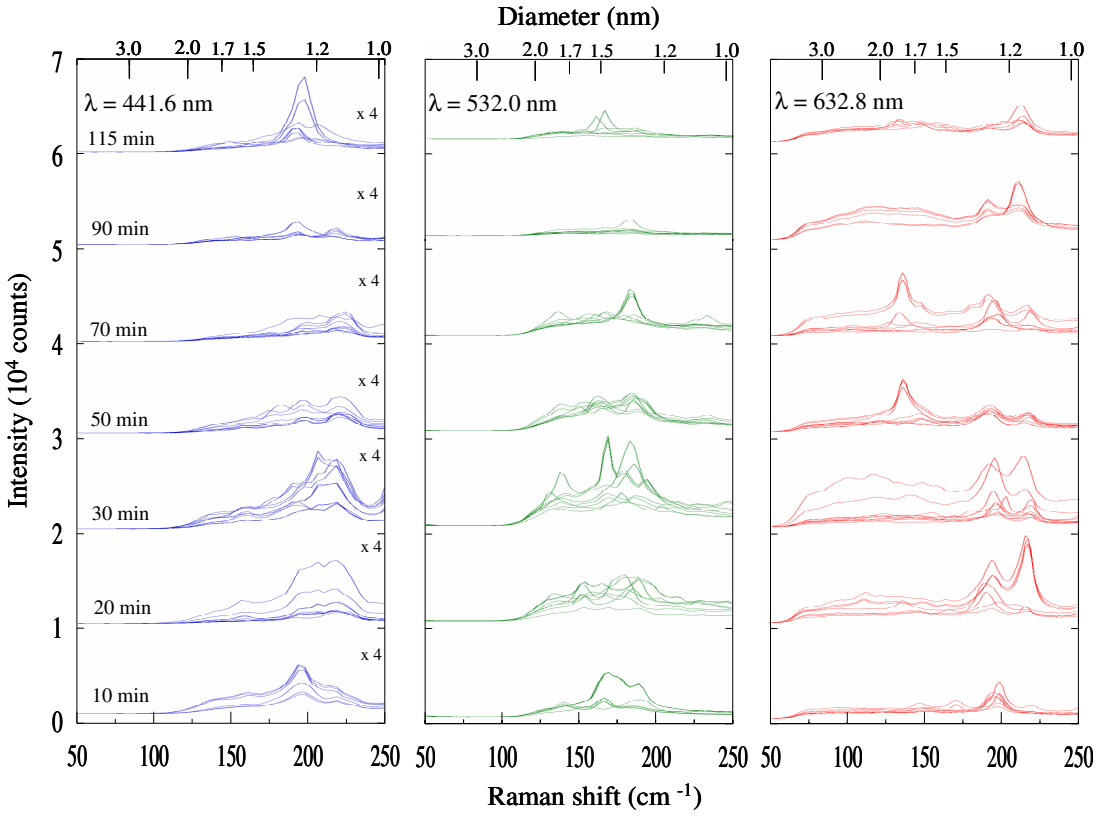
Diameter (nm)
3.0 2.0 1.7 1.5 1.2 1.0
λ = 441.6 nm
λ = 532.0 nm
λ = 632.8 nm
115 min
90 min
70 min
50 min
30 min
20 min
10 min
x 4
Intensity (10^4 counts)
Raman shift (cm -1)
0 1 2 3 4 5 6 7
50 100 150 200 250

Fig. 2

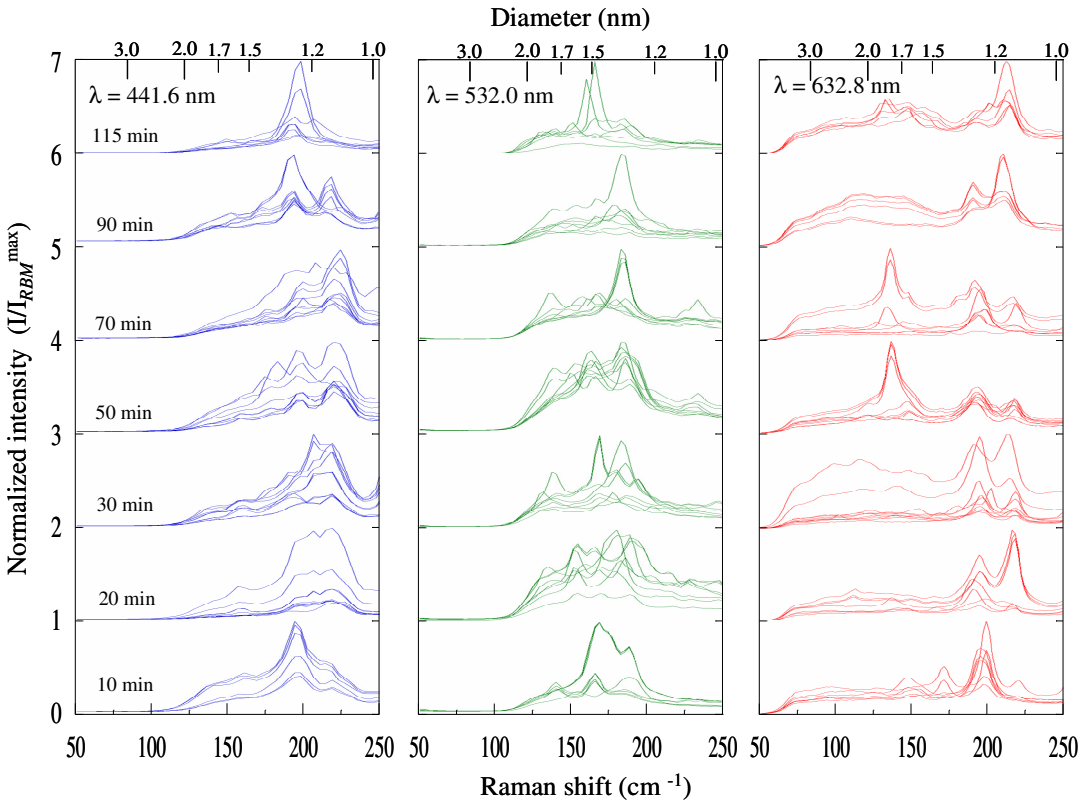
Diameter (nm)
3.0 2.0 1.7 1.5 1.2 1.0
λ = 441.6 nm
λ = 532.0 nm
λ = 632.8 nm
115 min
90 min
70 min
50 min
30 min
20 min
10 min
Normalized intensity (I/I_RBM^max)
Raman shift (cm -1)
0 1 2 3 4 5 6 7
50 100 150 200 250

Fig. 3

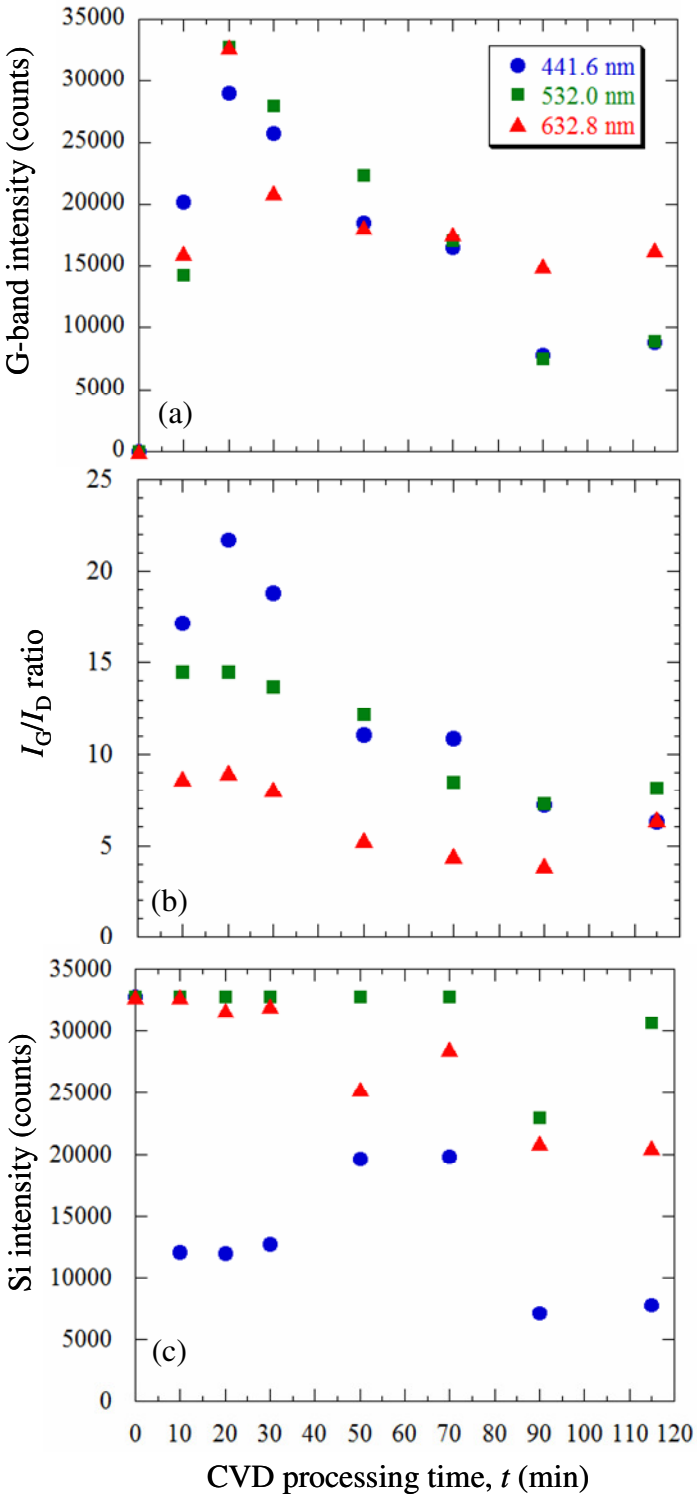
G-band intensity (counts)
35000
30000
25000
20000
15000
10000
5000
0
441.6 nm
532.0 nm
632.8 nm
(a)
I_G/I_D ratio
25
20
15
10
5
0
(b)
Si intensity (counts)
35000
30000
25000
20000
15000
10000
5000
0
(c)
0 10 20 30 40 50 60 70 80 90 100 110 120
CVD processing time, t (min)

Fig. 4

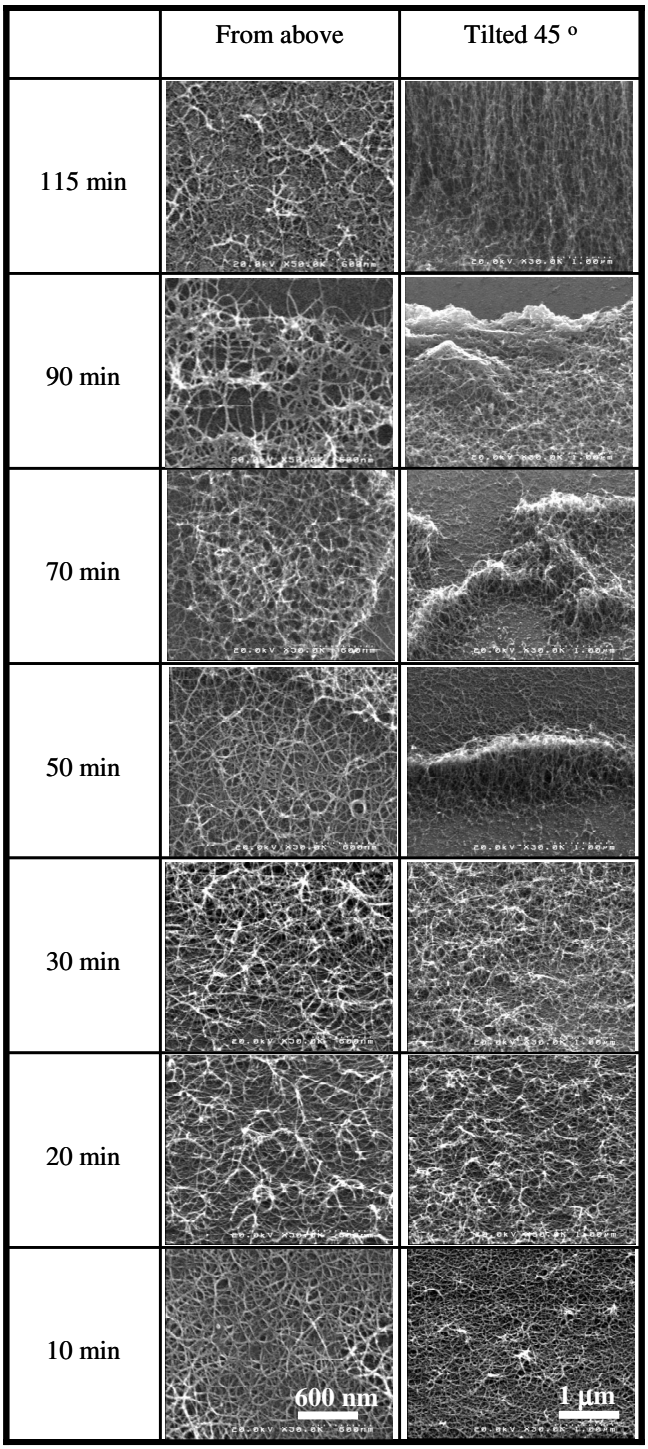
From above
Tilted 45 º
115 min
90 min
70 min
50 min
30 min
20 min
10 min
600 nm
1 µm

Fig. 5

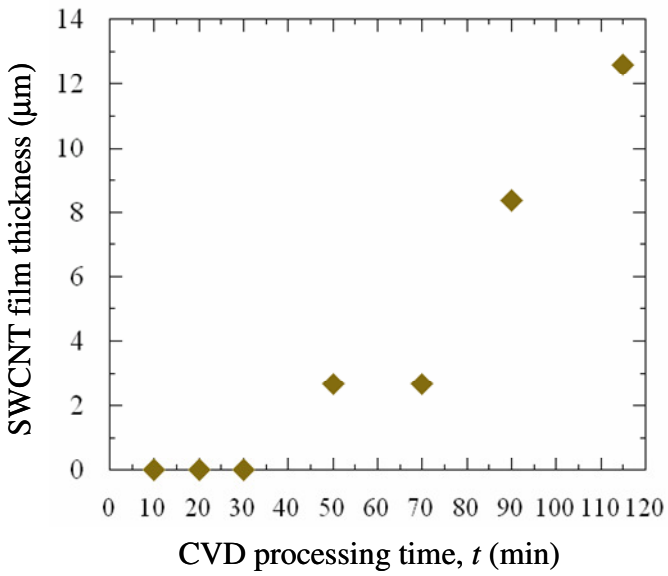
SWCNT film thickness (μm)
0
2
4
6
8
10
12
14
0 10 20 30 40 50 60 70 80 90 100 110 120
CVD processing time, t (min)

Fig. 6